Chapter 5

Competition between Cubic and Tetragonal Phase induced Unusual Vertical Magnetization Shift and Exchange Bias in $Co_xMn_{3-x}O_4$ ($1.00 \leq x \leq 2.00$) Spinel Nanoparticles

5.1 Introduction

In this chapter, we systematically study the structure dependent magnetic properties such as magnetic transitions, exchange bias and VMS in $Co_xMn_{3-x}O_4$ where x varies from 1.00 to 2.00. In section 5.2, evolution in the magnetic properties like transition temperatures (Tc_1 and Tc_2) and coercivity (H_C) are discussed with increase in x. M_{ZFC} corresponding to Tc_1 is found to be increased at the expense of M_{ZFC} corresponding to Tc_2, similar to the increase in cubic phase at the expense of tetragonal phase. We further discuss the spontaneous and conventional exchange bias, and establish a systematic relationship between the crystal structure and VMS, which is explained on the basis of interaction between different arrangements of spins in A and B sublattices, in section 5.3. The results of this chapter are summarized in section 5.4.

5.2 Magnetic Analysis

5.2.1 Temperature dependent magnetization

Temperature (T) dependent magnetization (M) of the $Co_xMn_{3-x}O_4$ (x = 1.00 to 2.00) nanoparticles is measured with an external applied magnetic field of 0.5 kOe in the temperature range of 3 to 300 K under zero field cooled (ZFC) and field cooled (FC) condition. **Figure 5.1(a)** shows the FC and ZFC magnetization curve for x = 1.00 to 1.50. With decreasing temperature from 300 to 5 K, ZFC Magnetization (M_{ZFC}) shows two peaks Tp_1 and Tp_2 for x = 1.00, 1.25 and 1.50, as shown in **Figure 5.1**. Tp_1 is observed at 136, 150, and 149 K for x = 1.00, 1.25, and 1.50, whereas Tp_2 is observed at 87, 88, 89

K, respectively. Further, the transition temperature is determined at the point where the tangent to the susceptibility peak intersects the extrapolation of the paramagnetic line parallel to the temperature axis. Thus, corresponding to the Tp_1 and Tp_2, two magnetic transition temperatures, Tc_1 and Tc_2 are observed **Figure 5.1(b)**. While Tc_1 is found to be 165, 170 and 165 K, Tc_2 is found to be 93, 97 and 101 K for x = 1.00, 1.25 and 1.50, respectively. Tc_1 corresponds to the transition from paramagnetic to a high temperature ferrimagnetic phase and Tc_2 refers to the transition from high to low temperature ferrimagnetic phase.

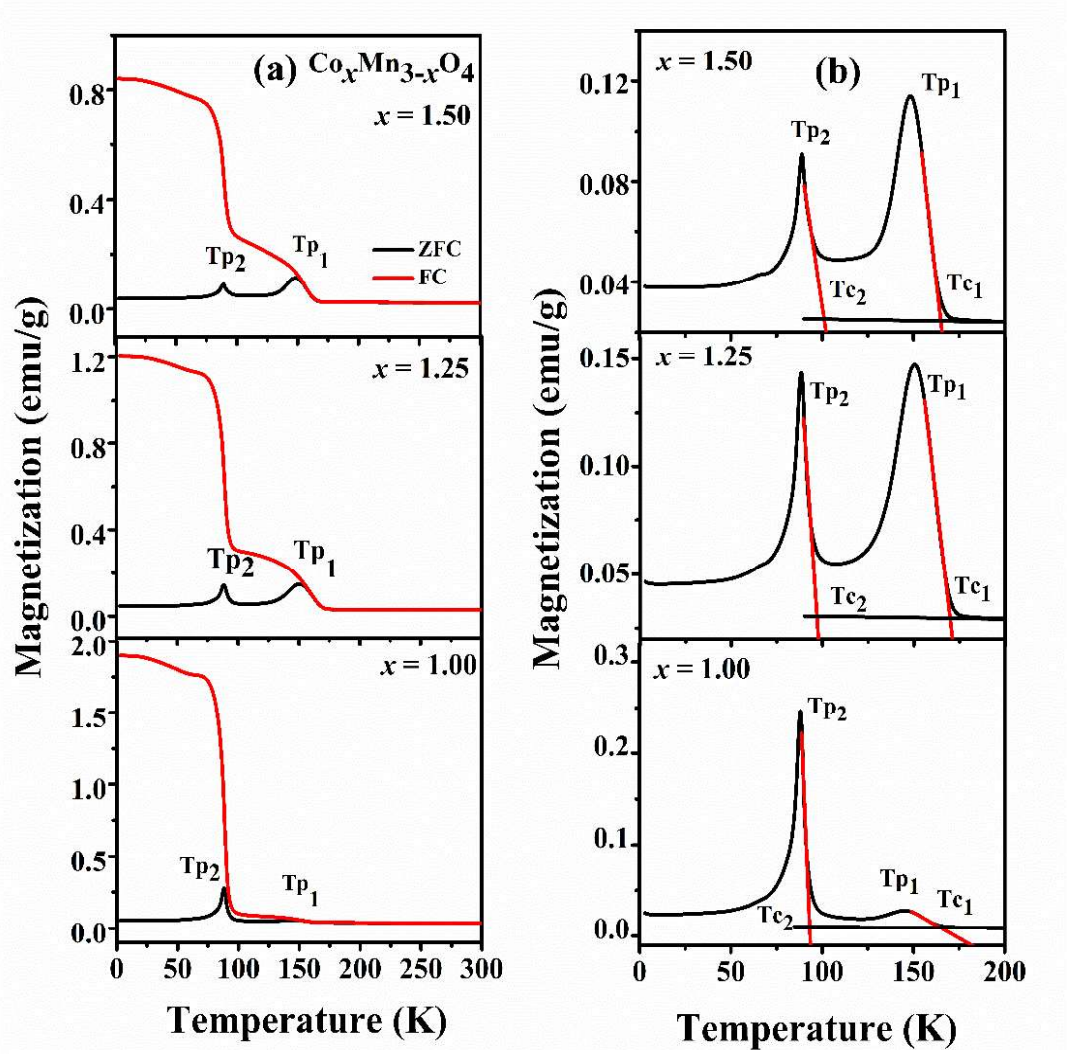

Figure 5.1: (a) FC-ZFC magnetization vs temperature, (b) enlarged view of ZFC peaks and transitions temprature by extrapolation method, for $Co_xMn_{3-x}O_4$ (x = 1.00, 1.25, 1.50) nanoparticles, measured at 0.5 kOe.

Figure 5.2(a) shows the FC and ZFC magnetization curve for x = 1.75 and 2.00. With decreasing temperature from 300 to 5 K, ZFC Magnetization (M_{ZFC}) shows only one peak Tp_1 at 154, and 148 K for x = 1.75 and 2.00, respectively. A single magnetic transition Tc_1 is revealed at 176 and 167 Kc for x = 1.75 and 2.00, respectively (**Figure 5.2(b)**).

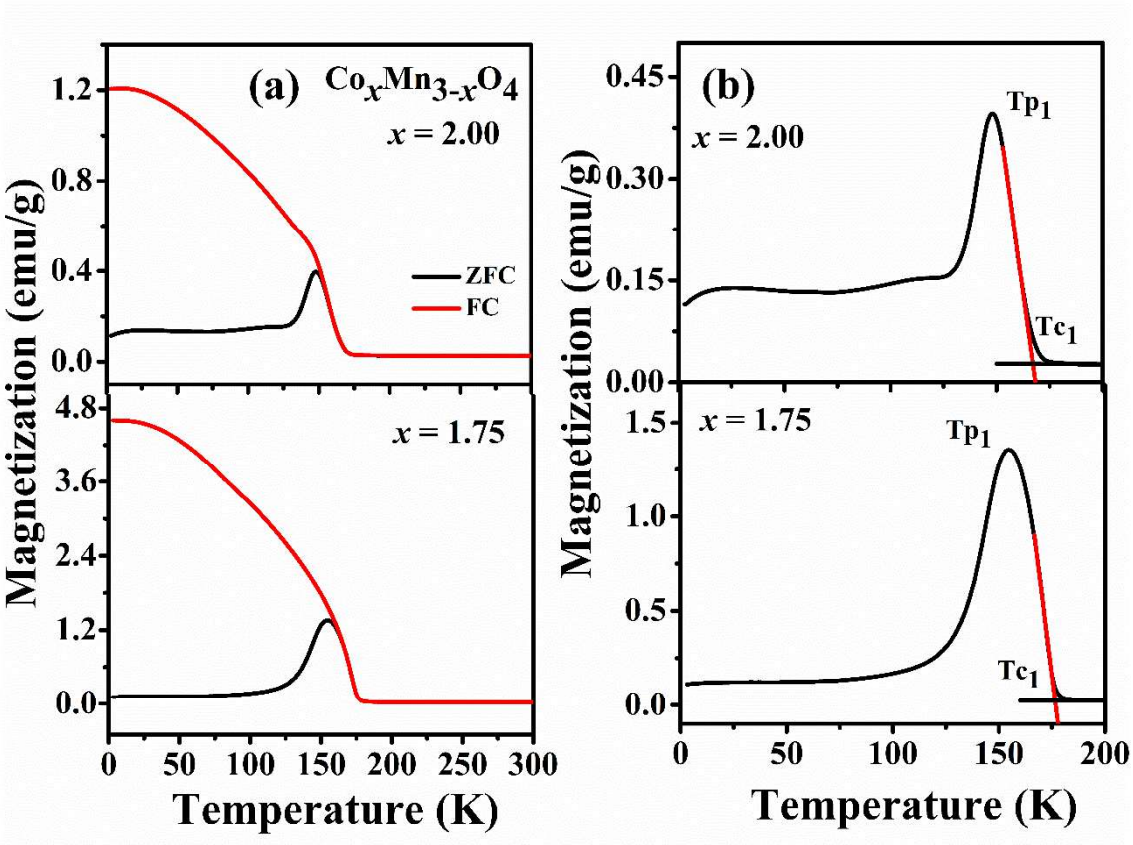

Figure 5.2: (a) FC-ZFC magnetization vs temperature, (b) enlarged view of ZFC peaks and transitions temprature by extrapolation method, for $Co_xMn_{3-x}O_4$ (x = 1.75, and 2.00) nanoparticles, measured at 0.5 kOe.

Further one can notice that for x = 1.00, M_{ZFC} corresponding to Tp_2 is higher than that of Tp_1. With increase in x, while M_{ZFC} at Tp_2 decreases, M_{ZFC} corresponding to Tp_1 increases. Surprisingly for x = 1.25, M_{ZFC} at Tp_2 and Tp_1 is almost equal and when x = 1.50, M_{ZFC} at Tp_1 dominates over M_{ZFC} at Tp_2 and for x = 1.75 and 2.00, no Tp_2 exists. Thus, it is clear that with increase in x, Tp_1 increases at the expense of Tp_2. In literature, for x = 1.00, it is dictated that Tc_1 is obtained due to some impurity phases associated with $Co_xMn_{3-x}O_4$ and Tc_2 is due to the existence of Yafet–Kittel (Y-K) spin structure [83,103,122]. However, we successfully show that cubic phase increases at the expense of tetragonal one with an increase in x which confirms that Tc_1 and Tc_2 correspond to the cubic and tetragonal phases, respectively. In chapter 3 [179], we have shown that for $CoMn_2O_4$ (x = 1), Mn^{3+} ions occupied by octahedral sites associated with Yafet–Kittel spin structures, whereas Co^{2+}/Mn^{2+} ions present in tetrahedral sites show the collinear behaviour in tetragonal phase [80,83]. Below Tc_2, majority of Mn^{3+} cations in the B sites attain a non-collinear triangular (Y-K) spin canting arrangement which lead to large ferrimagnetic moments. These noncollinear moments show vanishing effects among Mn^{3+} ions above Tc_2 due to which a decrement in magnetization is observed in M–T curve associated with small fraction of cubic phase [179]. In the present case, x = 1.00 having a dominating tetragonal structure exhibits a maximum M_{ZFC} corresponding to Tc_2. With increase in x, the tetragonal phase fraction decreases along with the Mn^{3+} ions at the B site and shows a decrease in M_{ZFC}. The cation distribution obtained from X-ray absorption fine structure analysis illustrates that Mn^{3+} and Co^{2+} ions mainly occupy B and A sites, respectively for x = 1.00. With increase in x, Co^{3+} replaces Mn^{3+} ions. Further, EXAFS shows the presence of Mn^{4+} ions instead of Mn^{3+} in B site when x is increased to 1.75 which is also supported by XPS. This specifies the collinear AFM spin arrangement rather than Y-K spins at B site. Hence, it confirms that M_{ZFC} at Tp_1 is associated with

collinear AFM arrangement at B site for the compositions having pure cubic phase. Furthermore, it is observed that the ZFC and FC curves overlap above Tp_1, indicating that the system is in equilibrium as a result of the fast fluctuations of the magnetic moments [80]. The observed complex behaviour accompanied by the competition of spin moments among the A and B sites could play an important role in measuring the magnetization with varying external magnetic fields at different temperatures.

5.2.2 Field dependent magnetization

Magnetization versus magnetic field measurement for $Co_xMn_{3-x}O_4$ (x = 1.00, to 2.00) has been performed at different temperatures within 300 to 5 K and in between the range of −60 to +60 kOe magnetic field. M-H curves for x = 1.00, 1.25 and 1.50, at the measuring temperature of 300, 150, 85, 50 and 5 K are shown in **Figure 5.3(a).** From the **Figure 5.3(a)**, presence of unsaturated hysteresis loops even at higher field for all temperatures is observed, confirm a strong signature of spin canting effect due to antiferromagnetic interactions among the constituent ions in two sub-lattices, nonlinear arrangement of spin and presence of anisotropy**.** This type of behaviour is commonly observed in spinel oxides like Mn_3O_4, $MgMn_2O_4$, $ZnMn_2O_4$ possessing Yafet–Kittel spin structures [158–160]. At room temperature, M-H curves for all the compositions are found to be linear due to the paramagnetic phase. For x = 1.00, 1.25 and 1.50, with decrease in the measuring temperature, the M-H loop area increases and become maximum for 50 K followed by a decrease and becomes minimum for 5 K. The coercive field H_C is calculated as $H_c = (|H_C^+| + |H_C^-|)/2$, where H_C^+ and H_C^- represent the fields of right and left branches of the hysteresis loop at M = 0 axis. H_C versus temperature behaviour is shown in **Figure 5.3(b)**. Coercivity starts to increase with lowering the temperature and reaching a maxima of 8.26, 6.09 and 6.45 kOe for x = 1.00, 1.25 and 1.50, respectively at 50 K which is below

Tp_2. Afterwards, H_C decreases and shows minimum values of 0.93, 3.74 and 1.38 kOe for x = 1.00, 1.25 and 1.50, respectively, at 5 K.

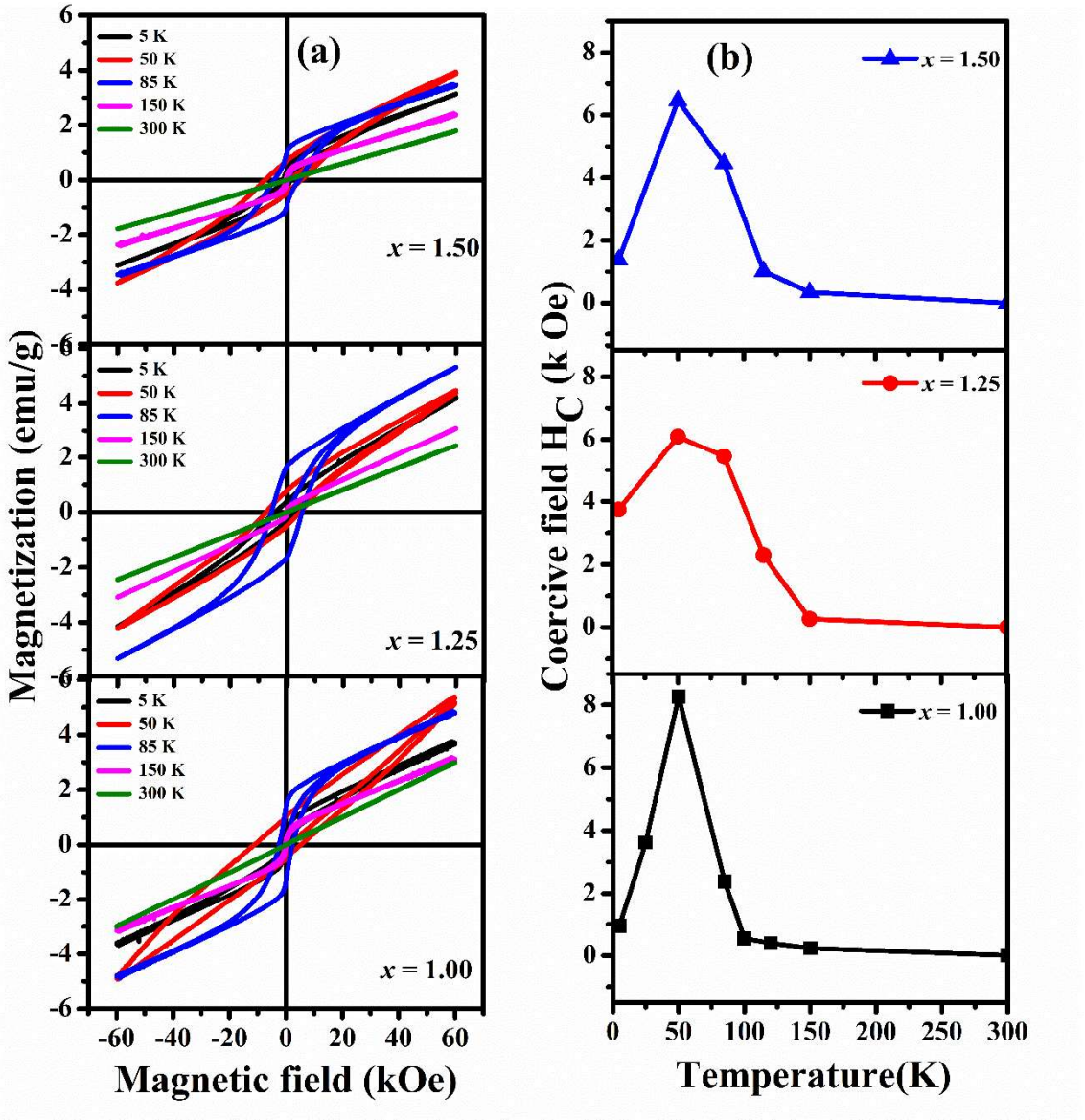

Figure 5.3: (a) ZFC Magnetization vs magnetic field hysteresis loops at various measuring temperatures, (b) H_C versus temperature behaviour, for $Co_xMn_{3-x}O_4$ (x = 1.00, 1.25, and 1.50) nanoparticles.

M-H curves and H_C versus temperature behaviour for x = 1.75 and 2.00, at the measuring temperature of 300, 150, 85, 50 and 5 K are shown in **Figure 5.4(a and b).** The M-H loop tends towards saturation in comparison to x = 1.00,1.25 and 1.50. Additionally, loop area continuously increases and found maximum at lower temperature (5 K) in contrast to x = 1.00,1.25 and 1.50, where the loop area is found to be increased at lower temperature **Figure 5.4(a)**. Coercivity increases continuously with decreasing temperature and attains a maximum H_C of 7.23 and 5.54 kOe for x = 1.75 and 2.00, respectively at 5 K as depicted in **Figure 5.4(b).** The obtained coercivity (H_C) and remanent magnetization (Mr) for all the samples are shown in **Table 5.1**.

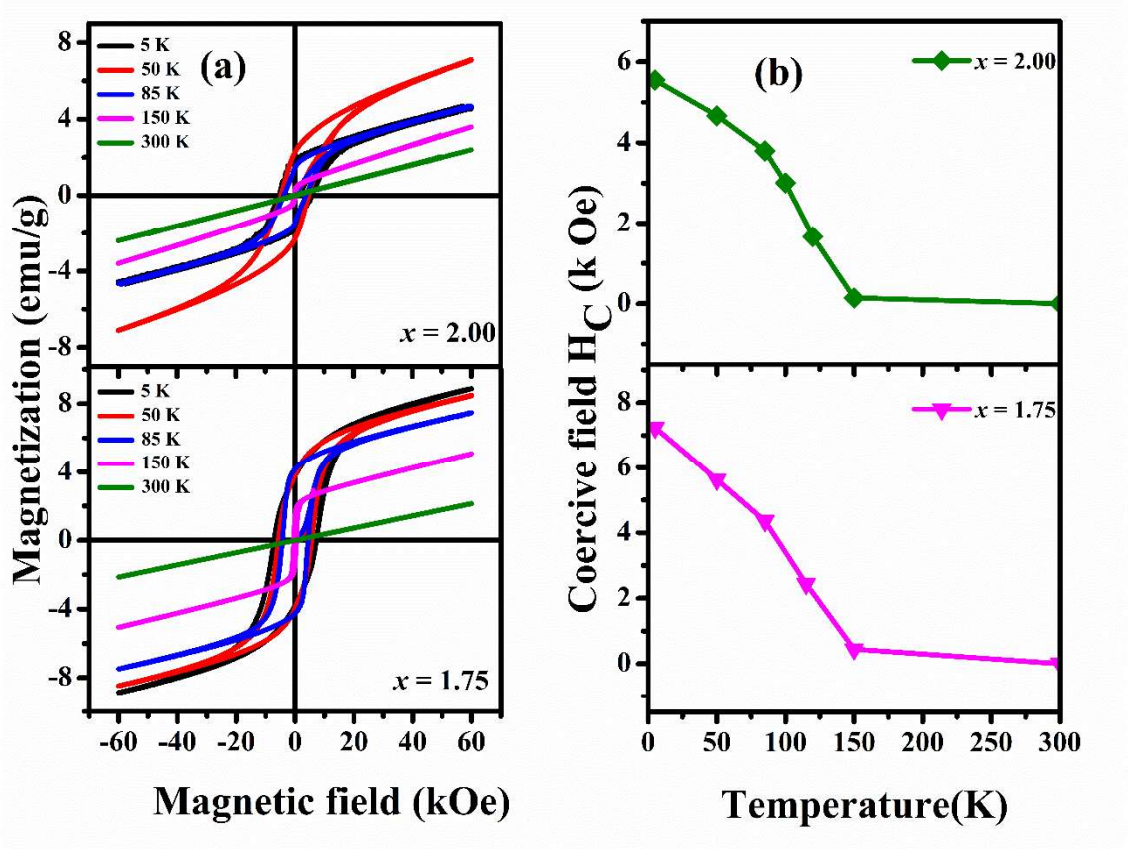

Figure 5.4: (a) ZFC Magnetization vs magnetic field hysteresis loops at various measuring temperatures, (b) H_C vs temperature behaviour, for $Co_xMn_{3-x}O_4$ (x = 1.75, and 2.00) nanoparticles.

For x = 1.00, 1.25 and 1.50, the coercivity trend with measuring temperature differs from the earlier reported trend for ferrimagnetic spinel. For these compositions M_{ZFC} shows the two transitions (Tc_1 and Tc_2) with two peak temperatures (Tp_1 and Tp_2). Following this, H_C shows temperature dependent behaviour. Coercivity starts to increase in the vicinity of Tc_1 (150 K). However, below Tc_2, a sharp enhancement in H_C is found and reaches the maxima at 50 K which is below Tp_2. Afterwards, H_C decreases and shows minimum values at 5 K. In contrast, coercivity follows the general ferrimagnetic behaviour with temperature in case of x = 1.75 and 2.00. M_{ZFC} shows a single magnetic transition, Tc_1 and peak temperature, Tp_1 corresponding to the pure cubic phase. Below Tc_1, the coercivity increases continuously with decreasing temperature and attains a maximum H_C at 5 K. An unusual decrement in H_C at lower temperatures is associated with tetragonal phase. Although such unusual H_C behaviour has not been found earlier for Co-Mn based spinel, Pandey et al. have reported such type of behaviour for chromite spinel and explain in terms of correlation between H_C and M_{ZFC} [49,83]. Continuous decrease in H_C with increase in temperature is reported by Szablewska et al. for $CoFe_2O_4$ single domain nanoparticle with different molecular surface coatings, which is not valid here [180]. In the present case, Mn^{3+} ions present in the B sites give rise to Yafet–Kittel spin structures, whereas cations occupying the A sites show the collinear ferromagnetic behaviour for tetragonal phase. It is thus confirmed that there are some interactions associated with Y-K spin structure which leads to the reduction in H_C below Tp_2 and induces such unusual behaviour for compositions having coexistence of tetragonal and cubic phases. The absence of Y-K spins (Mn^{4+} present instead of Mn^{3+}) in pure cubic phase leads to ideal behaviour of H_C.

Table 5.1: Coercivity and remanent magnetization for $Co_xMn_{3-x}O4$ (x = 1.00, 1.25, 1.50, 1.75 and 2.00).

S. No.	Temperature	x = 1.00		x = 1.25		x = 1.50		x = 1.75		x = 2.00	
		H_C (kOe)	Mr (emu g^{-1})	H_C (kOe)	Mr (emu g^{-1})	H_C (kOe)	Mr (emu g^{-1})	H_C (kOe)	Mr (emu g^{-1})	H_C (kOe)	Mr (emu g^{-1})
1.	5	0.926	0.355	3.738	0.365	1.376	0.313	7.233	3.77	5.547	1.828
2.	50	8.257	0.786	6.092	0.643	6.466	0.643	5.628	3.85	4.671	2.305
3.	85	2.375	1.355	5.435	1.647	4.460	0.970	4.359	4.15	3.798	1.45
4.	150	0.228	0.144	0.263	0.108	0.341	.1555	0.442	1.435	0.143	0.206
5.	300	0	0.045	0	0.004	0	.016	0	0.002	0	0.018

5.3 Conventional and Spontaneous Exchange bias and VMS

The unusual H_C behaviour with temperature, inspires to study the hysteresis behaviour after cooling under field irrespective to the composition. **Figure 5.5** depicts temperature dependent hysteresis (M-H) loops performed with field cooling (FC) and zero field cooling (ZFC) at 5 and 50 K for $Co_xMn_{3-x}O_4$ (x = 1.00 to 1.50). In ZFC condition, the a small asymmetricity observed along the magnetic field (H) axis in M-H curves is known as spontaneous exchange bias (H_{SEB}). However, in FC condition the shifting along the both magnetization axis and external field axis are noticed. While the former case is attributed to vertical magnetization shift (VMS), the latter is denoted by conventional exchange bias (H_{CEB}) [60]. From **Figure 5.5**, it is clear that the shift along magnetization axis continuously decreases with increase in x from 1.00 to 1.50. **Figure 5.6** depicts FC and ZFC M-H loops performed at 5 and 50 K for x = 1.75 to 2.00. Both the FC and ZFC loops show asymmetricity along the magnetic field (H) axis, however shifting along the

magnetization axis is found to be absent for these compositions. The exchange bias is estimated using the relation, $H_{EB} = |H_C^+ + H_C^-|/2$, where H_C^- and H_C^+ are the left and right coercive fields, where hysteresis curve intersects the magnetization axis [161]. On calculating the exchange bias using above relation the exchange bias is found to be overestimated, which is discussed later.

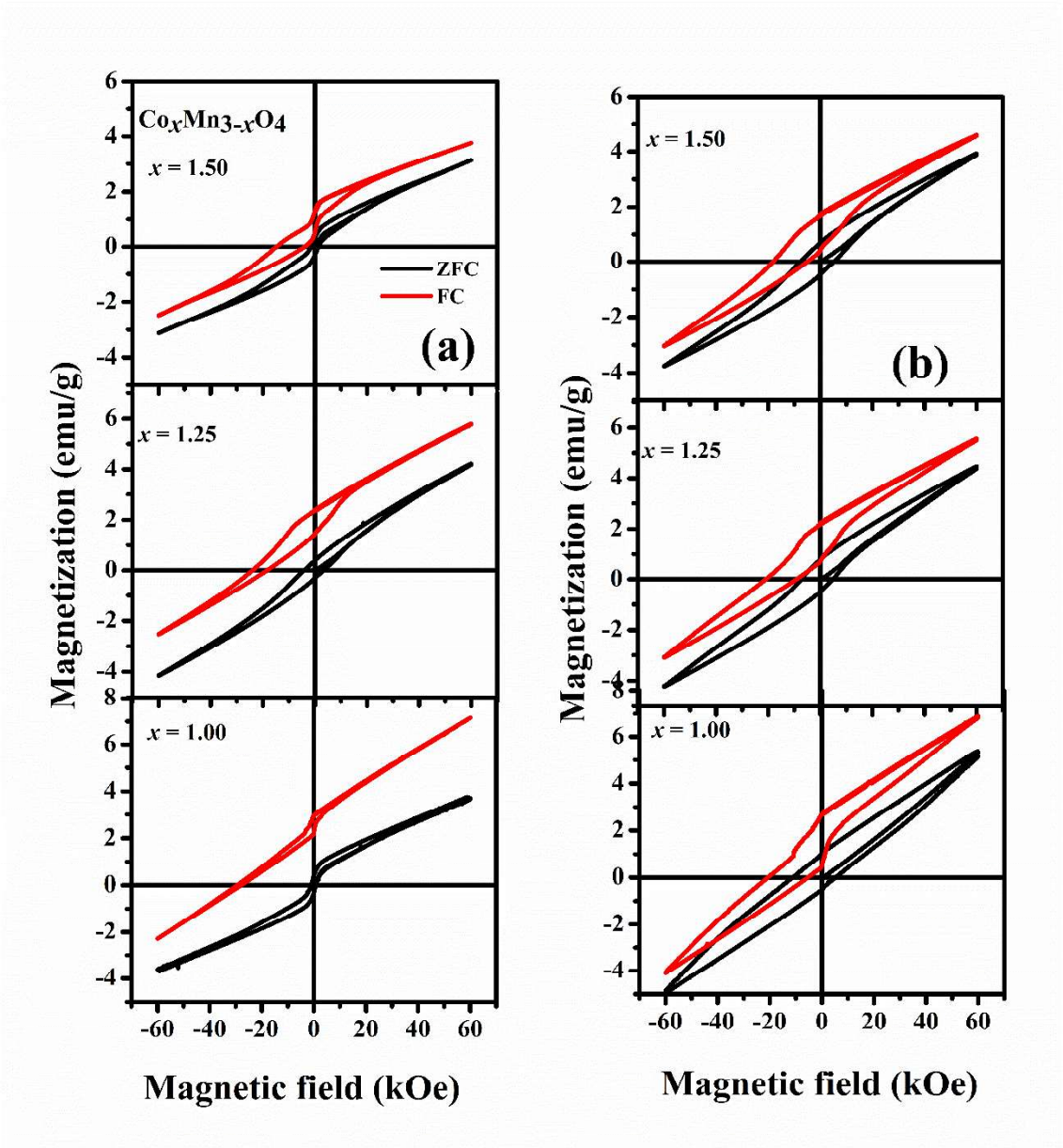

Figure 5.5: ZFC and FC M-H curve at, (a) 5 K and (b) 50 K for $Co_xMn_{3-x}O_4$, where x = 1.00, 1.25, 1.50.

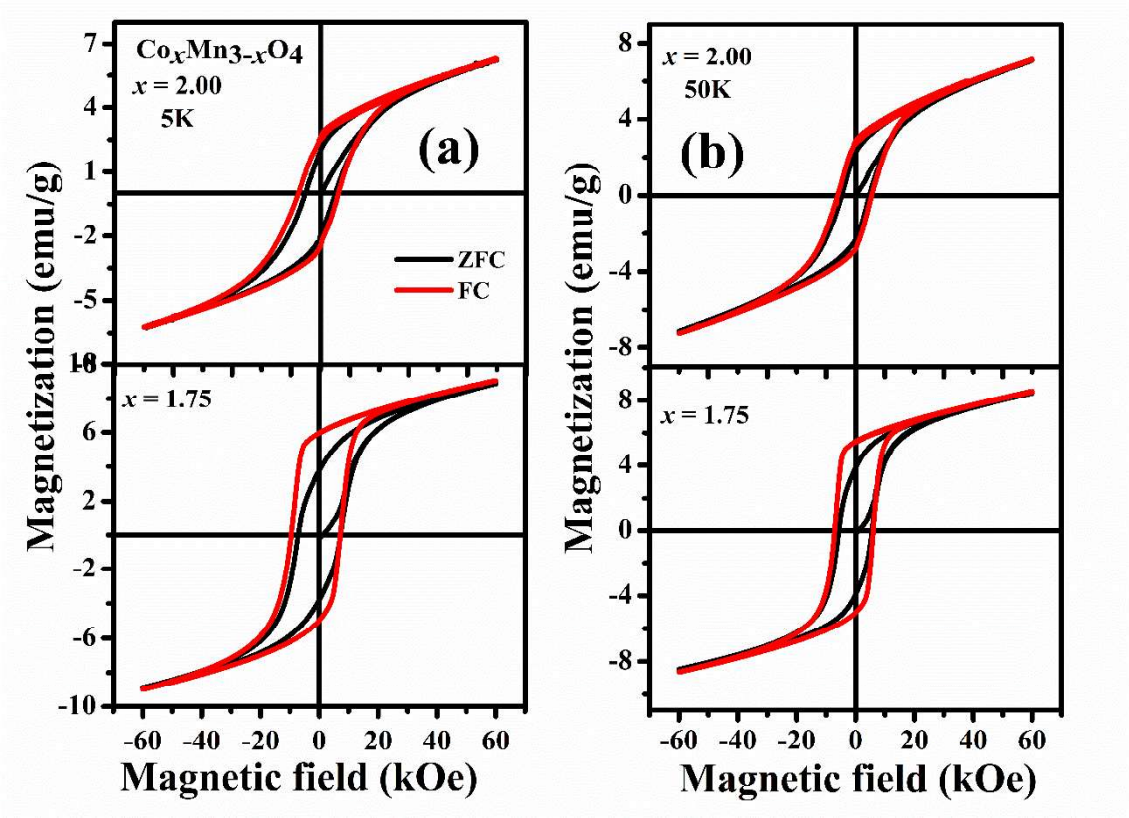

Figure 5.6: ZFC and FC M-H curve at, (a) 5 K and (b) 50 K for $Co_xMn_{3-x}O_4$, where x = 2.00, and 1.75.

Furthermore, the VMS is estimated using the relation $|M^+_{max} + M^-_{max}|/2$, where M^+_{max} and M^-_{max} are magnetizations at extreme positive and negative magnetic fields [59,162]. We report one order magnitude higher VMS than the previously reported VMS of 0.15 and 0.2 emu/g in $NiFe_2O_4$ and $NiCr_{1.7}Fe_{0.3}O_4$, respectively [61,161]. **Figure 5.7** shows a correlation between the composition dependent VMS and the tetragonal phase fraction estimated from structural analysis. It is observed that VMS is found to be higher at 5 K than 50 K for the composition having coexistence of both phases. At 5 K, VMS is found to be 2.5, 1.63 and 0.73 emu/g for x = 1.00, 1.25 and 1.50, respectively, while at 50 K, VMS of 1.39, 1.24 and 0.72 emu/g are observed for x = 1.00, 1.25 and 1.50, respectively. This indicates that VMS decreases with an increase in Co content. It is interesting to note that for x = 1.50, where both phases are equally present, VMS is also found to be approximately same for 5 and 50 K. Above x = 1.50, VMS is not observed even at low

temperature (i.e., 5 K). Such change in VMS with composition has not been reported so far in the literature. VMS observed in $NiCr_{1.7}Fe_{0.3}O_4$ is believed to be caused by the obstruction of the ferromagnetic moment's rotation at A sublattices by the uncompensated AFM moments at B sublattices [161], while in $NiFe_2O_4$, the presence of exchange coupling between the spin-glass like phase and the ferrimagnetic phase leads to the occurrence of VMS [61]. In the present case, it is evident that VMS is associated with tetragonal phase. $CoMn_2O_4$ (x = 1.00) with dominating tetragonal structure have a significant amount of Mn^{3+} ions occupying the B site accompanied with a non-collinear Y-K spin structure and exhibits maximum VMS. With increasing x, the tetragonal phase fraction decreases, and occupancy of Mn^{3+} at the B site also reduces and hence, shows a decrease in VMS. For $x \geq 1.75$, Y-K spins are significantly reduced due to the presence of Mn^{4+} and Co^{3+} in the B site, and VMS disappears.

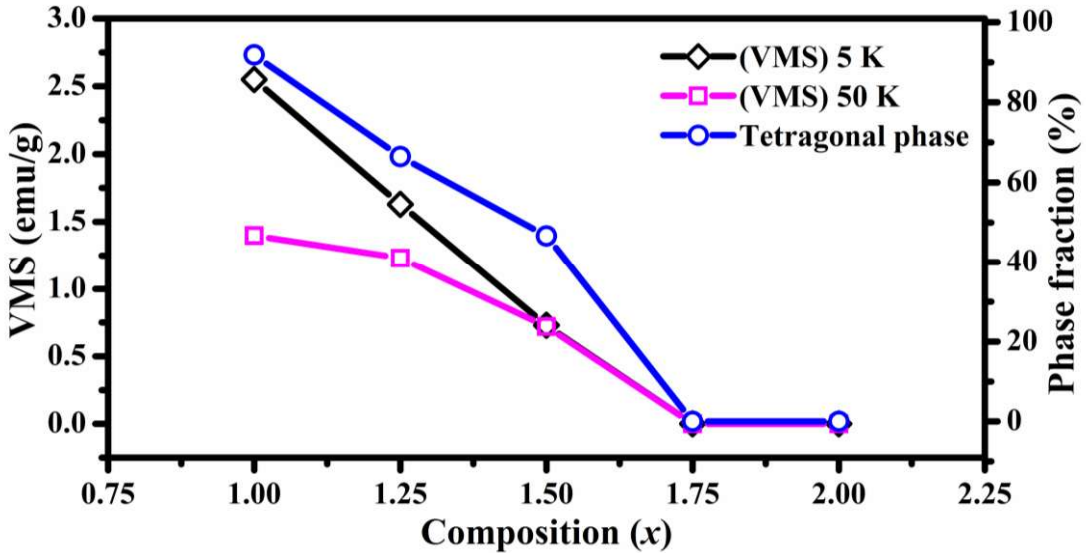

Figure 5.7: Variation with x, of VMS at 5 K and 50 K, and tetragonal phase fraction, for $Co_xMn_{3-x}O_4$, where x = 1.00 to 2.00.

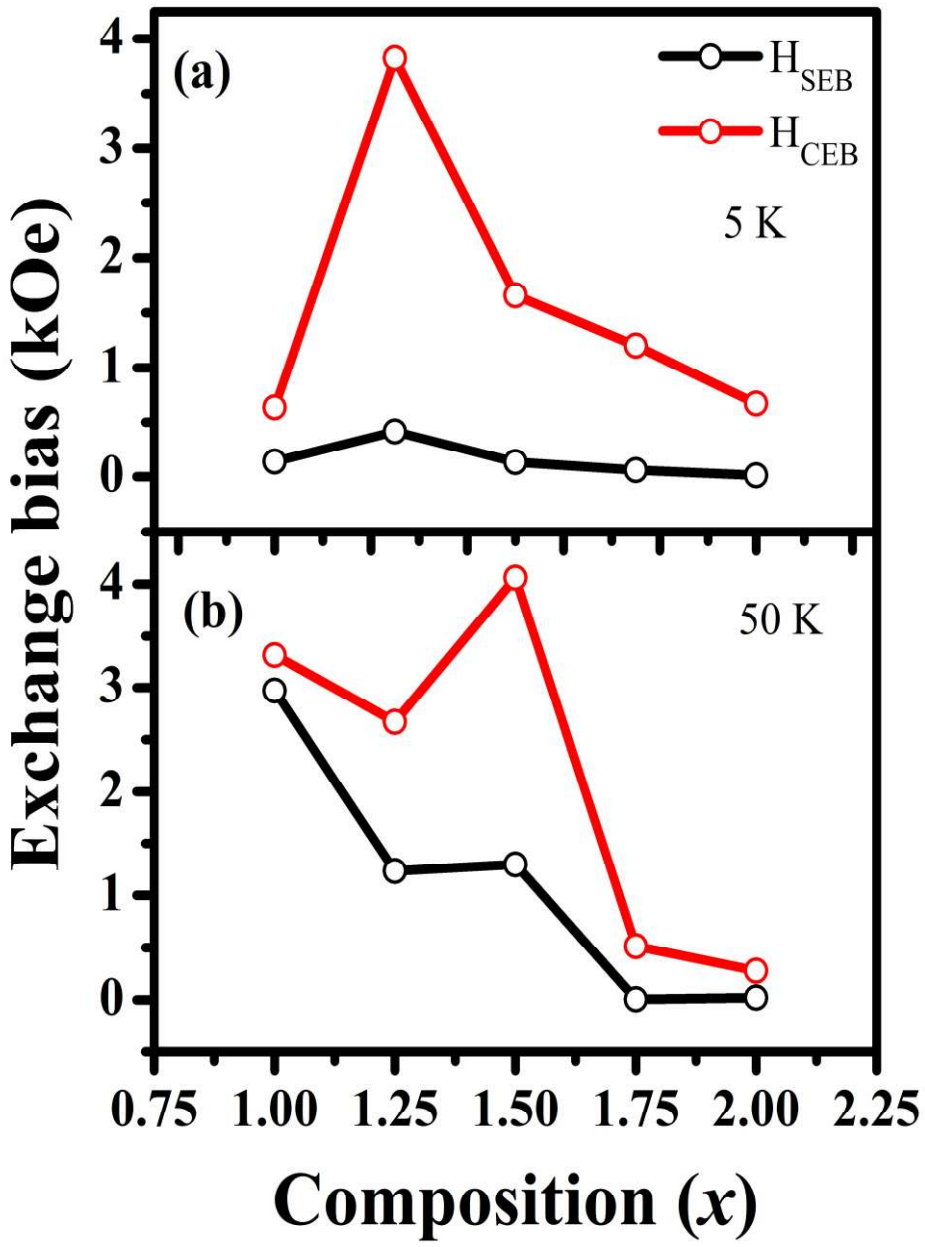

Figure 5.8: Variation in H_{SEB} and H_{CEB} with x at, (a) 5 K and (b) 50 K for $Co_xMn_{3-x}O_4$, where x = 1.00 to 2.00.

Further, we study the exchange bias effect with composition. The conventional exchange bias (H_{CEB}) is evaluated by measuring the M-H loop while cooling the sample in the presence of a magnetic field (10 kOe) to the desired temperature from room temperature. One may notice from **Figure 5.5(a)** that a very high H_{CEB} of 28.587 kOe for x = 1.00 is obtained at 5 K, which appears to be overestimated due to high irreversibility and non-saturation of magnetization during the hysteresis cycle. For accurate estimation,

we have subtracted the VMS from the M-H loop so that the hysteresis loop restores to its origin. After the correction, the composition dependent H_{SEB} and H_{CEB} at 5 K and 50 K are depicted in **Figure 5.8(a and b)**, respectively**.** It is observed that H_{CEB} is greater than H_{SEB} irrespective of the compositions and is found to be maximum for the composition with the coexistence of both phases. At 5 K, a maximum H_{CEB} of 3.822 kOe is obtained for $x = 1.25$, while at 50 K, maximum H_{CEB} of 4.062 kOe is observed for $x = 1.50$. Such trend gives evidence to the competition among A and B site spins for both phases which varies with the temperatures and the compositions.

Below transition temperature, under an external magnetic field of 60 kOe, the ferromagnetically (FM) ordered spins of the A sublattice and the uncompensated spins of the B sublattice align along the field direction. In contrast, reversing the direction of the applied magnetic field, while the FM-ordered spins flip in the field direction easily, the spins at the B sublattice remain unchanged. This exerts a pinning force on the reversible FM spins across the interface and exhibits exchange bias. Here, it is essential to mention that the Y-K spins at the B sublattice in the tetragonal phase provides a higher pinning force on the reversible FM spins across the interface than that in the cubic phase. Consequently, a high shift in the hysteresis loop along both field and magnetization direction is detected for the tetragonal phase, while in cubic phase, only the shift of the hysteresis loop along the field direction is observed. With increase in x, as the Mn^{3+} ions are decreased in B sublattice, the interaction between ferromagnetic spin in the A sublattice and uncompensated spins in the B sublattice varies accordingly [161]. For the coexistence of cubic and tetragonal phases, the exchange bias is high at a particular temperature and decreases rapidly when it is a pure cubic phase due to weakly pinned spins in the field direction for $x \geq 1.75$. However, VMS continuously decreases by x and disappears for $x \geq 1.75$. Therefore, one may conclude that while VMS is decided by the

tetragonality induced with the Mn^{3+} ions in B sublattice, which depends on *x*, the exchange bias originates from the interaction between differently arranged spins of the A and B sublattices for both the magnetic phases of $Co_xMn_{3-x}O_4$.

5.4 Conclusion

We reported the variation in magnetic properties in accordance with structural phases of $Co_xMn_{3-x}O_4$ with varying *x* from 1.00 to 2.00. Coexistence of tetragonal and cubic phase for $1.00 \leq x \leq 1.50$ and a pure cubic phase for $x > 1.50$ was observed in $Co_xMn_{3-x}O_4$. In accordance with two structural phases, for $x = 1.00$, two magnetic transitions Tc_1 and Tc_2 at 165 K and 93 K respectively were observed. With increase in *x*, M_{ZFC} corresponding to Tc_1 grew at the expense of M_{ZFC} corresponding to Tc_2 and finally at $x = 2.00$, only transition associated with Tc_1 was detected. Larger was the fraction of tetragonal phase, higher was the VMS. The maximum VMS of 2.5 emu/g was detected for $x = 1.00$. Although conventional and spontaneous exchange bias were evidenced irrespective of phase, a high H_{SEB} and H_{CEB} were obtained in compositions with coexistence of both tetragonal and cubic phase. It was concluded that the VMS was decided by the tetragonality induced by J-T active Mn^{3+} ions in the octahedral sublattice, however, exchange bias was controlled by the interaction between different spin arrangements of spins in A and B sublattices of $Co_xMn_{3-x}O_4$ which varied with temperature and composition.